

Effect of the Substitution Pattern of Diaminoanthraquinone on Some Physical Properties

M. Jamali,* J. C. Bernède,* and C. Rabiller†

*Groupe Couches Minces et Matériaux Nouveaux, EPSE, FSTN, Université de Nantes, 2 rue de la Houssinière, BP 92208, 44322 Nantes Cedex 3, France; and
†Laboratoire de Recherches en Biocatalyse, FSTN, Université de Nantes, 2 rue de la Houssinière, BP 92208, 44322 Nantes Cedex 3, France

Received January 6, 1998; in revised form May 25, 1998; accepted June 3, 1998

Two diaminoanthraquinones have been deposited under vacuum: 1,4-DAAQ and 2,6-DAAQ. They have been characterized by infrared (IR) absorption and nuclear magnetic resonance (NMR) to check that the products did not decompose during the deposition process. They have also been characterized by visible and near-ultraviolet absorption, X-ray diffraction (XRD), and X-ray photoelectron spectroscopy (XPS) and their purities have been checked by melting point measurements. The IR and NMR spectra of the films were identical to those of the reference powder spectra, which shows that the structure of the molecules is preserved. The presence of a hydrogen bond in 1,4-DAAQ is clearly put in evidence by the IR, NMR, XPS, and optical absorption measurements. Whereas 2,6-DAAQ thin films are crystallized, 1,4-DAAQ thin films are amorphous. The optical properties of 1,4-DAAQ thin films are modified by the presence of a silver thin film, whereas those of 2,6-DAAQ are not. © 1998

Academic Press

Key Words: organic compound; thin films; complex salt; silver; optical properties.

I. INTRODUCTION

Organic compounds are of current interest in many thin-film applications. More precisely, the enormous range of materials displaying a variety of electrical and optical properties, together with the ability to modify their physical and chemical properties, has led to an increasing research effort in this field. Organic thin films have been proposed for a wide variety of applications such as gas-sensitive chemistors (1), field effect transistors (FET) (2–5), optoelectronic devices (6, 7), electroluminescent diodes (LED) (8–10), and optical mass memories (11–13).

Among these materials, some anthraquinone derivatives (AQD), after complex-salt formation with a metal such as silver for instance, exhibit electrical and optical switching effects (14,15). Diaminoanthraquinones (DAAQ) are members of this promising family. The NH₂ substituent can interact with some foreign material to give complex salts with new electrical and optical properties. Recently, it has

been shown that complexation of 1,4-DAAQ with a metal organic metal salt may result in a coordination polymer (16). In the case of mass memory applications, thin films should be used. However, up to now, there are no detailed investigations on DAAQ thin films. Therefore, it is necessary to study systematically the properties of the DAAQ films and to compare them to those of the corresponding powder. Then the first attempts to obtain complex salt could be done.

In the present paper we have investigated two DAAQ compounds, 1,4-DAAQ, which exhibits a hydrogen bond, and 2,6-DAAQ, which does not. Properties related to the hydrogen bonds are investigated in some detail. Following this study, the modification of the optical properties of 1,4-DAAQ films in the presence of silver will be reported.

II. EXPERIMENTAL

II.1. Thin-Film Deposition Conditions

Films of diaminoanthraquinone with thickness ranging from 0.5 to 2 μm were deposited on substrates under a dynamic vacuum of 10⁻⁴ Pa by heating in a tantalum boat. Powders were provided by Aldrich with purity better than 97%. The structures of 1,4-DAAQ and 2,6-DAAQ are presented in Fig. 1.

The substrates used were polished glass, NaCl and KBr single crystals, and stainless steel slides. NaCl and KBr substrates were used for infrared (IR) and visible absorption studies, whereas the stainless steel substrates were used for X-ray photoelectron spectroscopy (XPS) analysis. During deposition, the substrate temperature, which was stabilized at 320 K, was monitored by a copper–constantan thermocouple attached with silver paste to the surface of the sample. To study the modification of the optical properties caused by Ag, thin films of silver were deposited on to DAAQ thin films without breaking the vacuum between the two evaporations. The evaporation rates and the film thickness were measured by the quartz vibration method. The thickness ratio t_{Ag}/t_{DAAQ} was about 0.2.

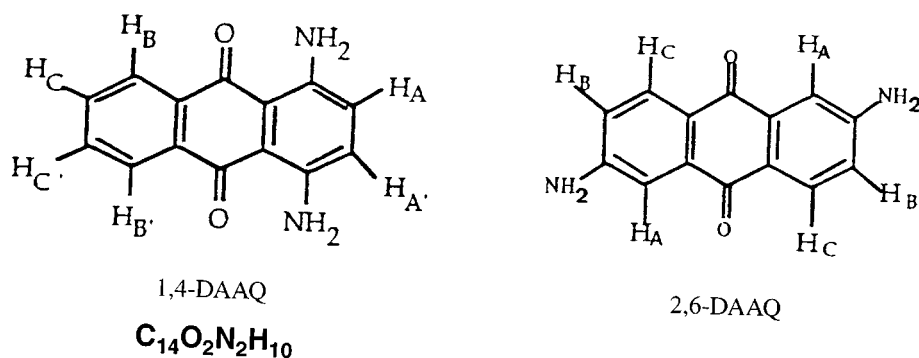


FIG. 1. Structures of the diaminoanthraquinones studied.

II.2. Sample Characterizations

DAAQ thin films and reference powder were identified by infrared, visible, and near-ultraviolet absorption and 1H NMR whereas the purity of the samples was checked by measuring their melting points. The films were chemically characterized further by XPS. X-ray diffraction studies (XRD) were also performed.

IR spectra were obtained with a Bruker IFS 85 FT-IR spectrometer.¹ Band positions are expressed in wavenumbers (cm^{-1}). Optical measurements were carried out with a Cary 2300 spectrophotometer from 2 to 0.2 μm .¹

1H -NMR spectra were recorded on a Bruker WM 250-MHz machine.² Tetramethylsilane (TMS) was used as internal standard and $CDCl_3$ as a solvent. Melting points were measured on a Kofler hot-stage apparatus and were uncorrected.

XPS analyses were performed with a Leybold LHS-12 apparatus.³ The data were obtained with a magnesium source of radiation (1253.6 eV) operating at 10 kV and 10 mA. The quantitative XPS studies were based on the determination of the C1s, N1s, and O1s peak areas with 0.2, 0.36, and 0.61, respectively, as sensitivity factors (the sensitivity factors are given by the manufacturer, Leybold). The spectrometer were used in mode PE. The decomposition of the XPS peaks into different components and the quantitative interpretation were made after subtraction of the background using the Shirley method (17). The developed curve-fitting programs permit the variation of parameters such as Gaussian/Lorentzian ratio, the full width at half-maximum (FWHM), and the position and the intensity of the contribution. These parameters were optimized by the curve-fitting program to obtain the best fit. To cancel the charge effect

¹Infrared, visible, and near-ultraviolet absorption measurements were carried out at the LPC-IMN.

²NMR measurements were carried out at the RMN and Chemical Reactivity Laboratory, FSTN.

³XPS measurements were carried out at the University of Nantes, CNRS.

related to the poor conductivity of the samples, the binding energy of the carbon-carbon bond present in the DAAQ has been taken as reference. In the literature (18) this band has a well-defined position at 285 eV.

III. EXPERIMENTAL RESULTS

III.1. Melting Points

The melting points of the different DAAQ powders are 595 and 535 K for 2,6-DAAQ and 1,4-DAAQ, respectively, whereas they are 598 and 537 K in the case of evaporated thin films. The values given by Aldrich for pure samples are 599 and 538 K; it can be seen that thin films give the best results. The melting point of organic compounds decreases with decreasing purity, and thin films are the purest samples. The deposition of the DAAQ thin films under vacuum is a very efficient process for purification of the compounds. It appears that nonvolatile impurities are excluded from the deposited thin films.

III.2. Absorption Spectroscopies (IR, Visible, Near-UV) and NMR

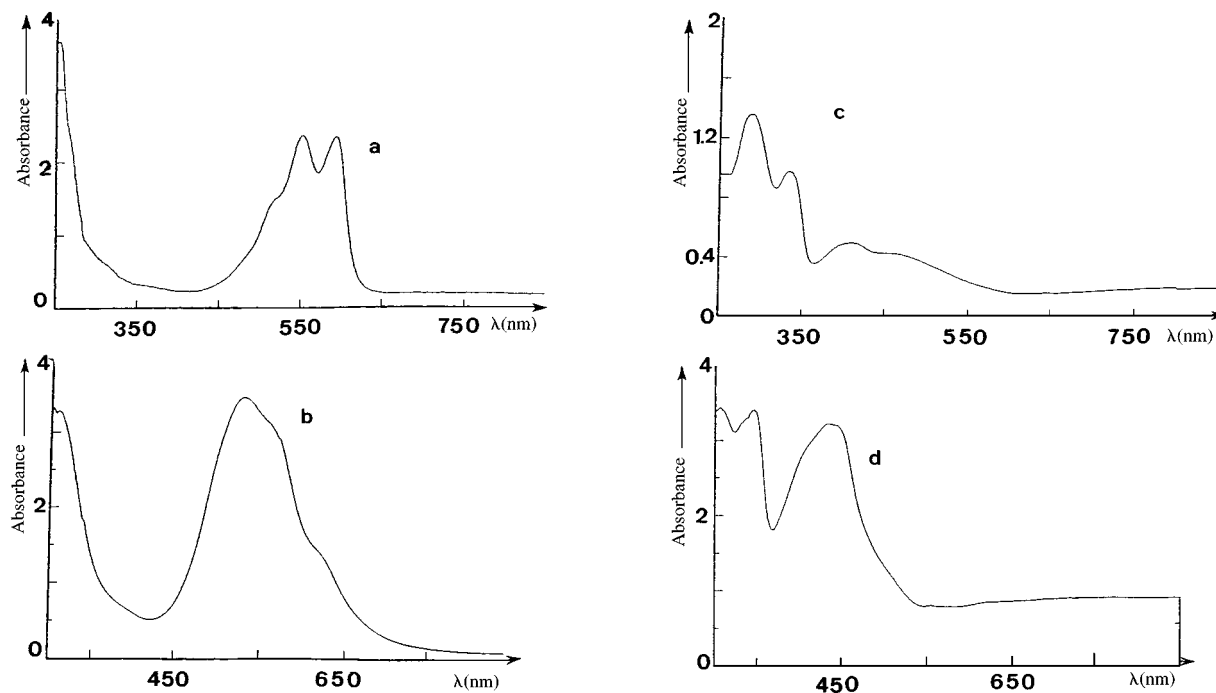
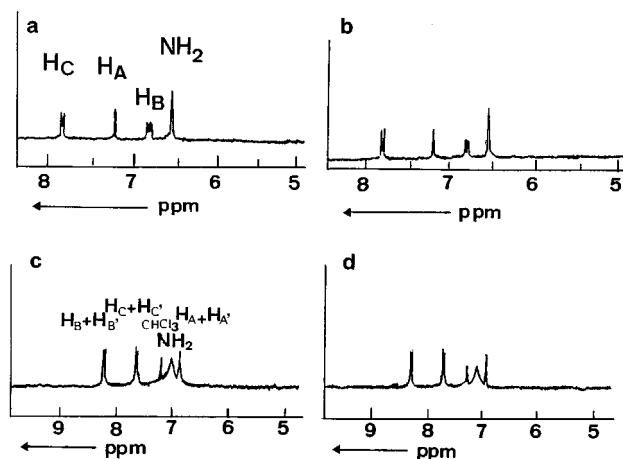
The IR spectra are summarized Table 1. It can be seen that there is no difference between absorption of the film and that of the corresponding powder. The attribution of the main absorption bands and the hydrogen bond influence will be discussed later.

The results obtained by NMR are reported in Fig. 2. In the case of the films, they were dissolved in $CDCl_3$ after removal from the substrates. The chemical shifts reported in Fig. 2 are measured with respect to TMS, and the nomenclature used is explicated in Fig. 1. Here also there is no difference between the films and the powders. Therefore, the IR and 1H -NMR results show that there is no deterioration of the DAAQ during the process of thin-film deposition. Moreover, as shown by melting point measurements, there is a purification of the starting materials.

TABLE 1
Characteristic IR Bands of the Different DAAQ Samples

Bonds	Wavelengths (cm ⁻¹)			
	1,4-DAAQ		2,6-DAAQ	
	Powder	Thin film	Powder	Thin film
C-H	723	723	749	749
	828	828	847	847
	1031	1031	886	886
	1125	1125	1081	1083
	1177	1178	1161	1162
C=C, C-C, C-N	1277	1279	1296	1296
	1404	1405	1330	1330
	1444	1445		
	1540	1539		
	1563	1563	1573	1569
NH ₂	1604	1604	1629	1629
C=O	1640	1643	1664	1664
NH ₂ '	3263	3275	3208	3211
	3385	3395	3334	3335
			3424	3425

The experimental optical absorption spectra are shown in Fig. 3. It can be seen that the spectra of the films are similar to those of the powder. However, it appears that in the case of 1,4-DAAQ there is a red shift effect of the whole spectrum


FIG. 3. Optical density spectra for (a) 1,4-DAAQ powder, (b) 1,4-DAAQ thin film (1 μm), (c) 2,6-DAAQ powder, and (d) 2,6-DAAQ thin film (1 μm).

FIG. 2. ¹H-NMR spectra for (a) 1,4-DAAQ powder, (b) 1,4-DAAQ thin film, (c) 2,6-DAAQ powder, and (d) 2,6-DAAQ thin film.

and a modification of the relative intensities of the different contributions of the broad band centered around 550 nm. Even in the case of 2,6-DAAQ the relative intensities are modified. An interpretation of these modifications will be proposed later.

III.3. XRD Study

Both DAAQ powders are crystallized (Figs. 4a and 4c). The diffraction peaks are in good accordance with the

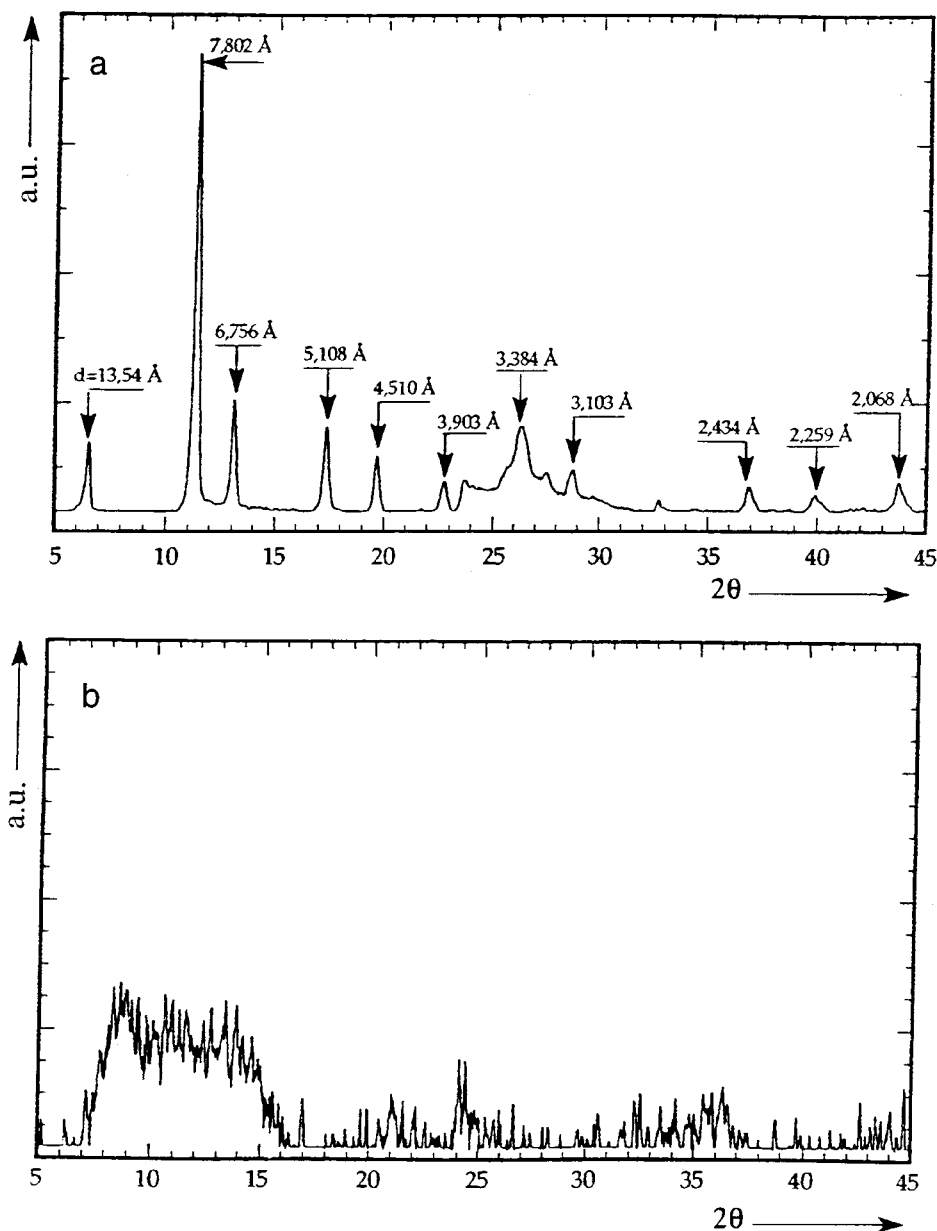


FIG. 4 X-ray diffraction patterns for (a) 1,4-DAAQ powder, (b) 1,4-DAAQ thin film (2 μm), (c) 2,6-DAAQ powder, and (d) 2,6-DAAQ thin film (2 μm).

reference given by the JCPDS data (No. 43-1682 in the case of 1,4-DAAQ). These results confirm that there is some order in the DAAQ powders.

In the case of the DAAQ thin films, there are strong modifications of the spectra.

The 1,4-DAAQ films appear to be amorphous (Fig. 4b), whereas if the 2,6-DAAQ films are crystallized (Fig. 4d), their diffractogram is quite different from that of the powder (Fig. 4c). Some diffraction peaks which are very weak in the diffractogram of the powder become very strong in the diffractogram of the films, which can be attributed to a

strong preferential orientation. Annealing at 343, 348, or 353 K for 24 or 36 h does not change the X-ray diffractograms of the films.

III.4. XPS Study

Quantitative XPS analysis of the DAAQ samples is reported in Table 2. The compositions of the films and of the powders are nearly the same. The small differences with the theoretical values can be attributed to surface contamination of the samples or instrumentation errors.

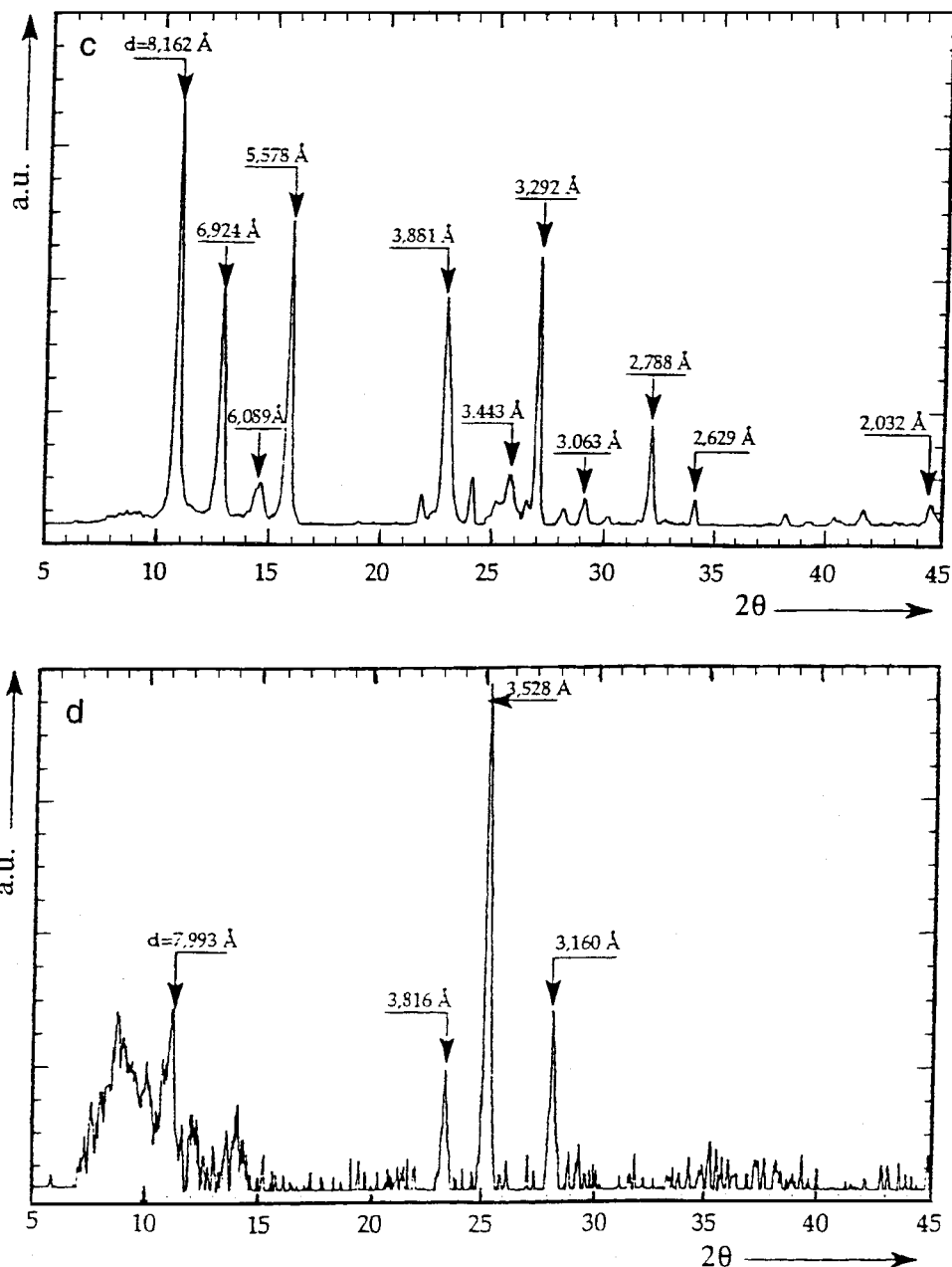


FIG. 4—Continued

The C1s peak (Fig. 5) can be decomposed into four contributions. The main component corresponds to the cyclic carbon (19), whereas the one situated at 286 eV can be assigned to the C–N bonds of the DAAQ. The third contribution can be attributed to the carbonyls (18) of the DAAQ. The weak fourth contribution may correspond to a small surface contamination (COOH); it may also be attributed to a shake-up effect ($\pi + \pi^*$), which is a classical effect in unsaturated organic compounds (20). The same decomposition is obtained whatever the sample is. This is not the case

for the N1s and the O1s peaks (Figs. 6 and 7). In the case of 2,6-DAAQ, only one component is needed to fit the experimental curve to the theoretical curve (Figs. 6b and 7b), whereas in the case of 1,4-DAAQ, the FWHMs of the N1s and O1s peaks are broader (Figs. 6a and 7a) and the O1s peak is anisotropic. In that case, the same shoulder is always observed on the high binding energy side; therefore two contributions are necessary to fit the experimental curve to the theoretical curve (Fig. 7a). These differences will be discussed shortly.

TABLE 2
Quantitative XPS Analysis of the Different DAAQ Samples
(at. %)

	Theoretical value	1,4-DAAQ		2,6-DAAQ	
		Powder	Thin film	Powder	Thin film
C	77.77	79	81	78	80
O	11.11	9	9	13	12
N	11.11	12	10	9	8

III.5. Optical Properties of the Ag/1,4-DAAQ Structures

As described in section II.2, Ag/DAAQ structures were deposited by evaporation under vacuum; however, it can be seen immediately in the case of 2,6-DAAQ that there was not any interaction between Ag and 2,6-DAAQ. The silver film remained unaltered on the glass substrate, only covered by the DAAQ film. In the case of the 1,4-DAAQ films after deposition, it was impossible to discriminate between the Ag and the DAAQ films because of their strong interdiffusion. Therefore Ag/1,4-DAAQ samples could only be studied by transmission measurements.

In Fig. 8 we can see that in the presence of silver a new absorption band appears around 400 nm, which is the classical energy domain of complex-salt absorption bands (16).

IV. DISCUSSION

As shown in the experimental results, there is no decomposition of the compounds during the thermal evapor-

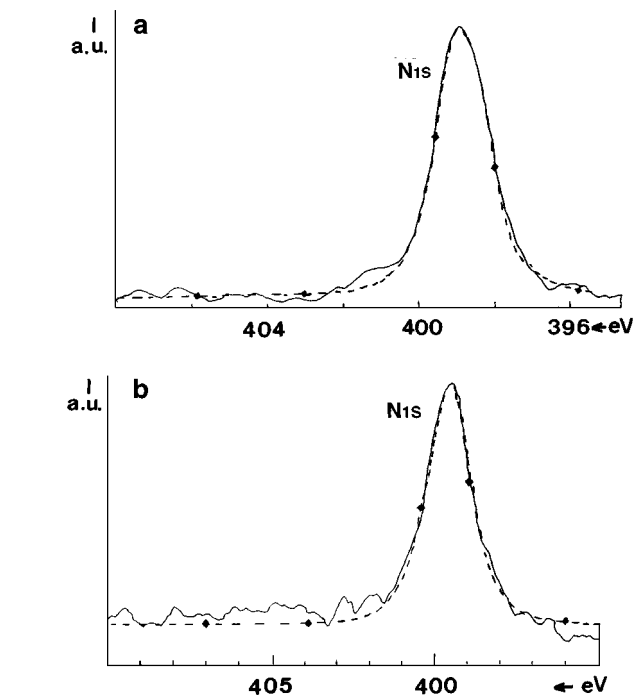


FIG. 6. Results of curve fitting to the N1s XPS peak: (—) experimental curve; (—●) fitted curve; (··●) different components. (a) 1,4-DAAQ thin film (2 μm); (b) 2,6-DAAQ thin film (2 μm).

ation process (Tables 1 and 2). It can be seen in Table 1 that, roughly, most of the vibrating frequencies are similar in the two DAAQ. However, by comparison with the 2,6-DAAQ spectrum, there are some peaks of 1,4-DAAQ which are shifted toward lower energy. In the IR spectrum of 2,6-DAAQ, the C=O stretching region is located at 1664 cm^{-1} ;

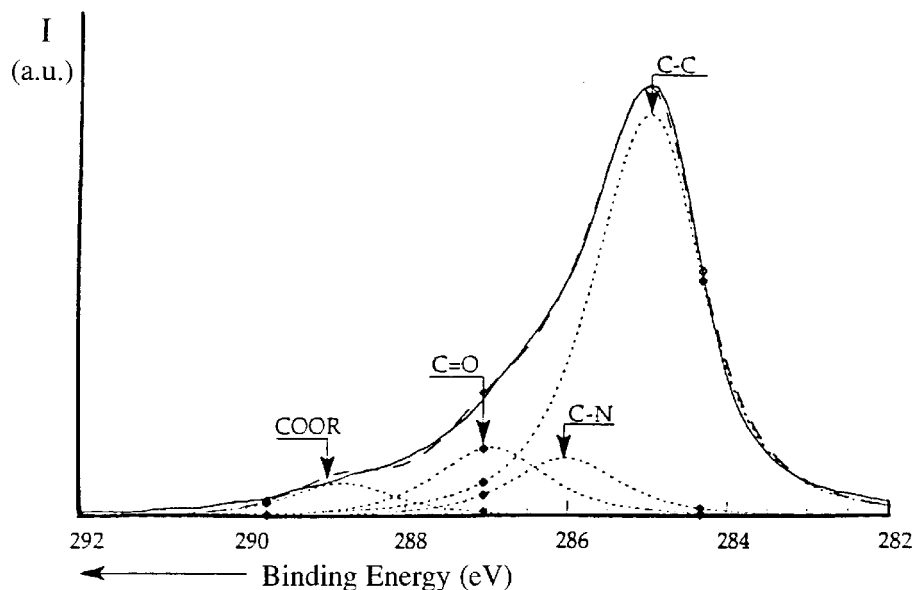


FIG. 5. Results of curve fitting to the C1s XPS peak of the 1,4-DAAQ thin film: (—) experimental curve; (—●) fitted curve; (··●) different components.

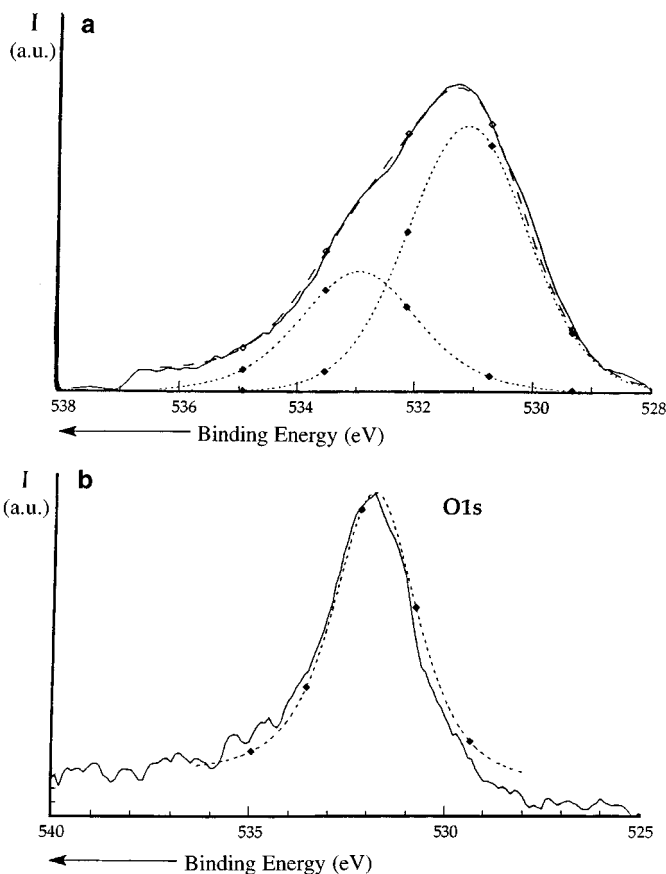


FIG. 7. Results of curve fitting to the O1s XPS peak: (—) experimental curve; (—●—) fitted curve; (··●) different components. (a) 1,4-DAAQ thin film (2 μm); (b) 2,6-DAAQ thin film (2 μm).

in the 1,4-DAAQ C=O is at 1640 cm^{-1} . Thus, the $\nu_{\text{C=O}}$ stretching vibration of 1,4-DAAQ is shifted to lower energy, an effect well known in hydrogen-bonded compounds (21). There is the same effect on the NH_2 vibrations (3424 and 3334 cm^{-1} in 2,6-DAAQ and 3385 and 3263 cm^{-1} in 1,4-DAAQ) (22).

The chemical shifts measured by NMR are reported in Fig. 2. The main difference consists in the shape of the signal attributed to the NH_2 protons. In the case of 1,4-DAAQ, the broad resonance peak ($\delta = 6.9\text{--}7.3$) gives evidence of a slow exchange (for the NMR technique). This corresponds to the hydrogen bond, which slows down hydrogen movement in NH_2 . In 2,6-DAAQ, this chemical shift corresponds to a narrow signal situated at $\delta = 7.5$, which excludes the presence of any hydrogen bond in that compound.

For XPS measurements the broadening of the O1s and N1s signals cannot be easily attributed to the charge density fluctuations on the nitrogen and the hydrogen atoms, fluctuations related to the hydrogen bond and the mesomeric effect present in the 1,4-DAAQ molecule (23) (Fig. 9). Usually only one form is measured with a charge intermediate between the two mesomeric formulas; however, an increase

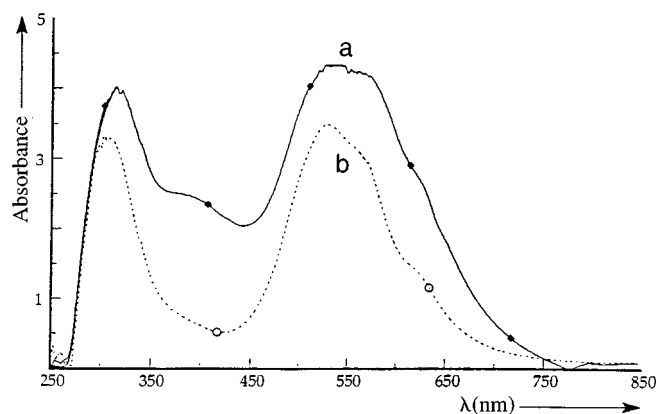


FIG. 8. Optical density spectra: (a) 1,4-DAAQ thin film (2 μm); (b) Ag/1,4-DAAQ thin-film structure (2 μm).

of the FWHM could be induced. Therefore if we assume that the N1s peak corresponds to only one peak, the FWHM is 1.7 in the case of 2,6-DAAQ and 2 in the case of 1,4-DAAQ. Moreover, in the case of the O1s signal of 1,4-DAAQ, two contributions are necessary. The second high-energy contribution is difficult to explain without the introduction of an extra contribution. The oxygen surface contamination is known to be situated at about 533 eV (19), which is in good agreement with a second oxygen contribution. Therefore it can be assumed that there is some surface contamination in the case of 1,4-DAAQ.

It has been shown (24–26) that the introduction of electron donor substituents on the benzene rings of the anthraquinone induces the appearance of new absorption bands, mainly in the visible domain. This effect can be seen in Figs. 3a and 3b. In the case of 1,4-DAAQ, two peaks are clearly resolved in this energy domain, which has been attributed (23) to the mesomeric effect present in this molecule (Fig. 9). As visible in Figs. 3c and 3d, the same effect is not present in the case of 2,6-DAAQ. It should be noted that even if a mesomeric structure is not excluded, its probability is far smaller in this molecule than in 2,6-DAAQ, because of the H bond present in the latter sample and not in the former. More precisely, even if the absorption band in the visible region of the spectrum could be attributed to resonance between the nucleus and the substituent in some of the disubstituted anthraquinones, there is evidence that this

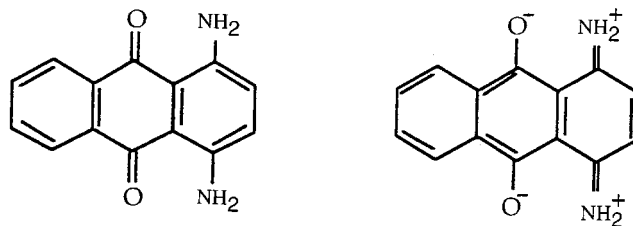


FIG. 9. Mesomeric effect in the 1,4-DAAQ molecule.

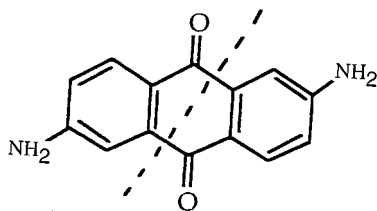


FIG. 10. Diagonal division of the 2,6-DAAQ.

band does not necessarily arise from the molecule as a whole. Thus the intensity for 1,8- or 1,5-disubstituted anthraquinone is twice that of the corresponding monosubstituted anthraquinone (24). This ratio shows that the band is associated with the conjugation of the substituent with the ketone group, the molecule being diagonally divided as in Fig. 10. In the case of 1,4-disubstituted anthraquinone, there is no such additivity because of interaction between the two chromophoric systems, which gives resonance (Fig. 9). This resonance induces the double-headed peak in the visible.

We have seen that if the molecules of the DAAQ are preserved during the evaporation, there are some differences between the XRD and the optical transmission spectra of the powders and the films, mainly in the case of 1,4-DAAQ. Since the films are deposited on a substrate, there could have been considerable tensile stress in them during the cooling of the films, which could broaden the absorption line width. Moreover, the disorder also induces a broadening effect. The strong disorder present in the 1,4-DAAQ films, which are amorphous, can also explain the shift of the absorption spectrum.

In the presence of silver, the large interdiffusion of the films facilitates interactions between the metal and the organic compound, which allows complex-salt formation as shown by the modification of the absorption of the 1,4-DAAQ. This interaction is facilitated by the absence of long-range order in these organic thin films. In the case of 2,6-DAAQ, there is long-range order since the films are crystallized and therefore their compactness forbids silver diffusion which decreases any interaction between silver and 2,6-DAAQ.

V. CONCLUSION

Following different characterizations of 1,4-DAAQ and 2,6-DAAQ thin films to check that the DAAQ did not decompose upon thermal deposition under vacuum, Ag/DAAQ samples were studied. The main differences between the properties of the two samples of DAAQ are linked with the hydrogen bond of 1,4-DAAQ.

Although there is no interaction between silver and 2,6-DAAQ, the optical properties of Ag/1,4-DAAQ thin-film samples are modified. The appearance of an absorption

band is very interesting for optical mass memory applications. These last samples are now under systematic investigations in our laboratory.

ACKNOWLEDGMENTS

The authors thank Mr. Assmann for performing XRD measurements. This work was supported by a contract between EEC and EPSE (Nantes, France) (Draft Contract ERBCII CT940070).

REFERENCES

1. M. A. Kervey, M. J. Schwing-Weill, and F. Arnaud, in "New Comprehensive Supramolecular Chemistry," (G. N. Gockel, Ed.), Vol. 1, 1996.
2. F. Garnier, R. Hajlaoui, A. Yassar, and P. Srivastava, *Science* **265**, 1684 (1994).
3. A. R. Brown, D. M. de Leeuw, E. J. Lous, and E. E. Havinga, *Synth. Met.* **66**, 257 (1994).
4. K. Pichler, C. P. Jarret, R. H. Friend, B. Rafer, and A. Moliton, *J. Appl. Phys.* **77**, 3523 (1995).
5. G. Guillaud, R. Ben Chaabane, C. Jouve, and M. Gamoudi, *Thin Solid Films* **258**, 279 (1995).
6. R. Reuter and H. Franke, *Appl. Phys. B* **48**, 219 (1989).
7. G. G. Malliaras, V. V. Krasnikov, H. J. Bolink, and G. Hadziioannou, *Appl. Phys. Lett.* **65**, 262 (1994).
8. E. I. Aminaka, T. Tsutsui, and S. Saito, *J. Appl. Phys.* **79**, 8808 (1996).
9. J. J. M. Halls, D. R. Baigent, F. Cacialli, N. C. Greenham, R. H. Friend, S. C. Moratti, and A. B. Holmes, *Thin Solid Films* **276**, 13 (1996).
10. M. S. Weaver, D. G. Lidzey, T. A. Fisher, M. A. Pate, D. O'Brien, A. Bleyer, A. Tajbaksh, D. D. C. Bradley, M. S. Skolnick, and G. Hill, *Thin Solid Films* **273**, 39 (1996).
11. J. J. M. Hartmann, M. A. Lind, and M. Mansuripur, *SPIE J.* **1078**, 308 (1989).
12. J. M. Haller and N. E. Iwamoto, *SPIE J.* **889**, 21 (1988).
13. R. C. Hoffman and R. J. Potember, *Appl. Opt.* **28**, 1417 (1989).
14. Y. Suzuki, A. Kawana, and J. Yamada, *Thin Solid Films* **150**, 175 (1987).
15. J. C. Bernède, M. Jamali, T. Ben Nassrallah, and A. Conan, *Ann. Chim. Fr.* **19**, 435 (1994).
16. K. Alagesan and A. G. Samuelson, *Synth. Met.* **87**, 37 (1997).
17. D. A. Shirley, *Phys. Rev. B* **5**, 6219 (1972).
18. G. Beamon and D. Briggs, "High Resolution XPS of Organic Polymers: The Scienta ESCA 300 Database." John Wiley and Sons, Chichester, 1992.
19. D. Briggs and M. P. Seah, in "Practical Surface Analysis. Auger and X-ray Photoelectron Spectroscopy," 2nd ed., Vol. 1, p. 543 Wiley, New York, 1990.
20. B. Aguis and M. Froment, "Surfaces Interfaces et Films Minces. Observation et Analyse". Dunod, Bordas, Paris, 1990.
21. G. C. Pimentel and A. L. McClellan, "The Hydrogen Bond." W. H. Freeman, and Company, San Francisco, 1960.
22. D. Lin-Vien, N. B. Colthup, W. G. Fateley and J. C. Grasselli, "The Handbook of Infrared and Raman Characteristic Frequencies of Organic Molecules," 1991.
23. A. Allen, B. Wilson, and C. Frame. *J. Org. Chem.* **7**, 169 (1942).
24. R. H. Peters and H. Sumner, *J. Chem. Soc.* 2101 (1953).
25. N. V. Platonova, K. R. Popov, and L. Vsmirnov. in "Nature of the Bands in the Electronic Absorption Spectra of Anthraquinone Dyes", pp. 357-363, 1968.
26. Yu. Yu. Yakolev, R. N. Nurmukhametov, V. G. Klimenko, and N. N. Barashkov, *J. Appl. Spectrosc.* **53**, 930 (1990).